


RESEARCH ARTICLE

On the time-frequency symbol density of FBMC/QAM systems

Mohammad Towliat | Seyyed Mohammad Javad Asgari Tabatabaee 

Department of Electrical Engineering,
Ferdowsi University of Mashhad,
Mashhad, Iran

Correspondence

Seyyed Mohammad Javad Asgari
Tabatabaee, Computer and Electrical
Engineering Department, University of
Torbat Heydarieh, Torbat Heydarieh, Iran.
Email: jasgarit@gmail.com

Summary

Filter bank multicarrier (FBMC) systems suffer from an inherent interference, which needs to be eliminated at the detection process. Orthogonal frequency division multiplexing/offset quadrature amplitude modulation (OFDM/OQAM) is a well-known FBMC system, which transmits real-valued symbols. In OFDM/OQAM, the time and frequency spacing between adjacent transmitted symbols are organized such that the inherent interference becomes pure imaginary and can be removed by a real-taking operation. Although OFDM/OQAM provides the maximal bandwidth efficiency, it falls short in handling the spatial multiplexing techniques in multi-input multi-output channels. In this regard, those modified FBMC systems, which transmit complex QAM symbols (FBMC/QAM) are used to support the spatial multiplexing techniques. In this article, we present a novel matrix formulation for the FBMC/QAM transmission procedure. On the basis of this presentation, we show that the maximal achievable time-frequency symbol density of FBMC/QAM, with the ability of perfectly removing the interference, is equal to that of the primer OFDM/OQAM.

KEYWORDS

FBMC/OQAM, FBMC/QAM, MIMO, spatial multiplexing, symbol density

1 | INTRODUCTION

In recent years, the surging usage of communication devices results in a huge data traffic demands.^{1,2} In this regard, the research subjects, such as big data mining and wireless sensor networks, have attracted lots of attentions. The achievements in this fields witnessed remarkable progress to address the confronted traffic issues.³⁻⁵ On the other hand, besides these concerns, in the next generation of wireless networks, novel transmission strategies, such as multicarrier systems, are developed to overcome the physical challenges of communication channels. Filter bank multicarrier (FBMC) schemes have attracted a lot of interests because of their flexibility for future communication applications.⁶⁻⁸ Also, Amini et al⁹ illustrated that FBMC can be a promising scheme for harsh and time-variant links, such as underwater acoustic channels. It is remarkable that the main feature of FBMC is to use well-localized prototype pulse shapes to control the intrinsic interferences.^{10,11} Well-localized pulse shaping also makes FBMC robust against interference originated from the time and frequency asynchronous users.¹⁰ Although the transient intervals of the well-localized pulse shape in FBMC lead to additional latency issues, this system is studied as the basis of the next generations of communication networks because of its prevailing advantages.^{12,13}

Orthogonal frequency division multiplexing/offset quadrature amplitude modulation (OFDM/OQAM) is one of the prevalent FBMC systems, which can provide the maximal bandwidth efficiency.^{10,14} To achieve this aim, in OFDM/OQAM

real-valued symbols are transmitted with overlapped pulse shapes in both time and frequency domains. The pulse shaping and time-frequency spacing between adjacent symbols are organized such that the interference on the desired real-valued symbol is pure imaginary and can be eliminated easily by a real-taking operation.¹⁰ Using no guard interval to transmit the symbols, the bandwidth efficiency of OFDM/OQAM is more than that of the cyclic prefix (CP) OFDM.

It must be noted that in the presence of nonideal channels, the receiver of the OFDM/OQAM system, firstly, needs to eliminate the channel effects on the received symbols before taking the real part.¹⁵ Because of this preliminary equalization, the application of spatial multiplexing (SM) along with the OFDM/OQAM system is a challenging issue. The reason is that those OFDM techniques to achieve the full diversity gain of multi-input multi-output (MIMO) channels are aborted when OFDM/OQAM is directly applied to them.¹⁶

Instead of real-valued symbols, transmitting complex symbols with the same procedure of OFDM/OQAM is 1 solution of the mentioned issue. On the other side, the resulted interference among the complex symbols becomes very large, which must be eliminated by using an appropriate transmission constellation at the transmitter and/or equalizers at the receiver. There are a range of FBMC systems, which transmit complex QAM symbols, and in this article, we call them the FBMC/QAM schemes.

It is noticeable that to compare the spectral efficiency of FBMC/QAM systems, the symbol density in time-frequency lattice is introduced. It implies the ratio of the number of transmitted data symbols (with the ability of perfectly removing the interferences at receiver) to the given time-frequency area.¹⁷ Note that transmitting complex symbols in FBMC/QAM leads to an enlarged interference among the symbols and, as a result, more complicated strategies are needed to eliminate this interference, compared with OFDM/OQAM. In this article, we investigate the time-frequency symbol density of FBMC/QAM. To this end, the contributions of this paper are summarized as follows:

- We first present a closed-form matrix formulation for FBMC/QAM procedure by considering some redundant transmitted symbols at the transmitter.
- On the basis of the matrix presentation, we prove that the transmission matrix of FBMC/QAM is rank deficient, such that half of its eigenvalues are ones and the other half are all zeros.
- According to the rank deficiency of the transmission matrix, we argue that the maximal achievable symbol density of FBMC/QAM, with the ability of completely removing the interference, is equal to that of the conventional OFDM/OQAM system transmitting real-valued symbols.

The remainder of this paper is organized as follows. In the next section, the OFDM/OQAM system model is reported. In Section 3, the transmission procedure of FBMC/QAM is presented in a matrix form. In Section 4, the maximum achievable time-frequency symbol density of FBMC/QAM is discussed. The related works are provided in Section 5, and finally, Section 6 contains the article's conclusions.

Notations: Matrixes, vectors, and scalar quantities are denoted by boldface uppercase, lowercase with an upper bar, and normal letters, respectively. $(\mathbf{A})_{n,p}$ is the entry in the n th row and p th column of matrix \mathbf{A} . Also, $\mathbf{A}^{(n,q)}$ is a square submatrix of \mathbf{A} in the n th row and q th column. \mathbf{I}_L and $\mathbf{0}_L$ are the identity and zero matrixes of the size $L \times L$, respectively. The Dirac delta function is denoted by $\delta_{k,l}$. $K = \text{kron}(\mathbf{A}, \mathbf{B})$ returns the Kronecker tensor product of \mathbf{A} and \mathbf{B} matrixes. Finally, the superscripts $(\cdot)^T$, $(\cdot)^H$, and $(\cdot)^*$ indicate transpose, conjugate transpose, and conjugate operators, respectively.

2 | OFDM/OQAM SYSTEM MODEL

Consider an OFDM/OQAM system with L subchannels. The transmitted signal in discrete-time form can be presented as

$$s[m] = \sum_k \sum_{l=0}^{L-1} d_{k,l} e^{j\pi(k+l)/2} f_{k,l}[m], \quad (1)$$

where $f_{k,l}[m] \triangleq f[m - kN_0] \exp(j2\pi l F_0 m)$ and $f[m]$ is the impulse response of the prototype filter. Also, $d_{k,l}$ is the real-valued symbol transmitted at the k th time instance and l th subchannel, which is multiplied by the staggered factor $\exp(j\pi(k+l)/2)$. Note that N_0 and F_0 are the spacing interval between 2 adjacent symbols in time and frequency domains, respectively. To achieve the maximum time-frequency symbol density, in OFDM/OQAM, $N_0 = L/2$ and $F_0 = 1/L$. Also, in OFDM/OQAM, the following orthogonality condition must be satisfied^{10,11}:

$$\operatorname{Re} \left\{ e^{-j\pi(\Delta k + \Delta l)/2} \sum_{m=-\infty}^{\infty} f_{k,l}[m] f_{k+\Delta k, l+\Delta l}^*[m] \right\} = \delta_{\Delta k, \Delta l}. \quad (2)$$

When the transmitted signal $s[m]$ passes through the ideal (distortion-free) channel and after addition of the noise components, the received signal becomes

$$y[m] = s[m] + w[m], \quad (3)$$

where $w[m]$ is the additive white noise. The demodulated symbol at the k' th time instance and l' th subchannel can be extracted by matched filtering the received signal $y[m]$ as

$$\begin{aligned} y_{k',l'} &= \sum_{m=-\infty}^{\infty} y[m] \left(e^{-j\pi(k'+l')/2} f_{k',l'}^*[m] \right) \\ &= \sum_k \sum_{l=0}^{L-1} d_{k,l} e^{-j\pi(\Delta k + \Delta l)/2} \sum_{m=-\infty}^{\infty} f_{k,l}[m] f_{k',l'}^*[m] + \varpi_{k',l'}, \end{aligned} \quad (4)$$

where $\Delta k \triangleq k' - k$, $\Delta l \triangleq l' - l$ and $\varpi_{k',l'} \triangleq \sum_{m=-\infty}^{\infty} w[m] (e^{-j\pi(k'+l')/2} f_{k',l'}^*[m])$ is the matched filter output noise. Since $f[m]$ is a normalized pulse shape, such that $\sum_{m=-\infty}^{\infty} |f_{k',l'}[m]|^2 = 1$, (4) can be rewritten as

$$\begin{aligned} y_{k',l'} &= d_{k',l'} \\ &+ \underbrace{\sum_{k \neq k'} \sum_{\substack{l=0 \\ l \neq l'}}^{L-1} d_{k,l} e^{-j\pi(\Delta k + \Delta l)/2} \sum_{m=-\infty}^{\infty} f_{k,l}[m] f_{k',l'}^*[m]}_{I_{k',l'}} \\ &+ \varpi_{k',l'}, \end{aligned} \quad (5)$$

where $I_{k',l'}$ is the interference term generated by the symbols at the other time instances and subchannels. According to (2), $I_{k',l'}$ is a pure imaginary term and the receiver can remove it easily by using a real-taking operator

$$\hat{d}_{k',l'} = \operatorname{Re} \{ y_{k',l'} \} = d_{k',l'} + \operatorname{Re} \{ \varpi_{k',l'} \}. \quad (6)$$

As it is mentioned before, in OFDM/OQAM, the maximal spectral efficiency is achieved by setting the time and frequency spacing to $N_0 = L/2$ and $F_0 = L/2$, respectively. To evaluate the spectral efficiency, the measure of time-frequency symbol density is defined as $D \triangleq 1/N_0 F_0$, which is ratio of the number of transmitted symbols to the given time-frequency area. Thus, in the case of OFDM/OQAM, $D = 2$ for real-valued symbols, which is equivalent to $D = 1$ for complex symbols. According to the Balian-Low theorem, this is the maximum achievable symbol density in a multicarrier scheme.¹⁸ Despite its maximum symbol density, OFDM/OQAM has a significant drawback. When the channel is nonideal, to detect a desired real-valued symbol, the receiver needs to get rid of the channel effects before the real-taking operation. This procedure can be performed with either a zero forcing or minimum mean square error equalizer.¹⁹ Due to the preliminary equalization, in MIMO channels, those SMs of OFDM cannot be directly applied to OFDM/OQAM.^{10,25}

In this regard, to eliminate the real-taking operation, and consequently, the preliminary equalization, the FBMC/QAM systems, which transmit complex symbols instead of real ones, are of the interest. In FBMC/QAM systems, the MIMO channel diversity gain can be fully achieved by applying SM techniques. On the other side, to cancel the enlarged interference of the FBMC/QAM system, some solutions are reported in Renfors et al and Lin et al.^{20,23} In these articles, to avoid the interference, 1 type of guard interval is considered between the transmitted symbols, which leads to the degradation of symbol density. The purpose of our article is to investigate the maximal time-frequency symbol density, which can be achieved in an FBMC/QAM system, with the ability of completely removing the interference. In this regard, in the following section, we first introduce a new matrix presentation of the FBMC/QAM procedure.

3 | MATRIX PRESENTATION OF FBMC/QAM

At the first step, let us suppose that the symbol $d_{k,l}$ is complex. Accordingly, we consider the $1/\sqrt{2}$ factor to normalize the symbol power equivalent to that of OFDM/OQAM. Also, for more facility, we can remove the staggered factor from (1),

and without loss of generality, the FBMC/QAM transmitted signal is presented as

$$s[m] = \frac{1}{\sqrt{2}} \sum_k \sum_{l=0}^{L-1} d_{k,l} f_{k,l}[m]. \quad (7)$$

Therefore, the demodulated symbol after the matched filtering becomes

$$y_{k',l'} = \frac{1}{2} \sum_k \sum_{l=0}^{L-1} d_{k,l} \sum_{m=-\infty}^{\infty} f_{k,l}[m] f_{k',l'}^*[m] + \omega_{k',l'}, \quad (8)$$

where $\omega_{k',l'} \triangleq 1/\sqrt{2} \sum_{m=-\infty}^{\infty} w[m] f_{k',l'}^*[m]$ is matched filter output noise. We can represent (8) as

$$\begin{aligned} y_{k',l'} &= \sum_k \sum_{l=0}^{L-1} \xi_{k'-k, l'-l}^{k'} d_{k,l} + \omega_{k',l'} \\ &= \sum_{\Delta k=-\infty}^{\infty} \sum_{\Delta l=-L+1}^{L-1} \xi_{\Delta k, \Delta l}^{k'} d_{k'-\Delta k, l'-\Delta l} + \omega_{k',l'}, \end{aligned} \quad (9)$$

in which $\Delta k \triangleq k' - k$ and $\Delta l \triangleq l' - l$. Also, the time-frequency interference extension at time instance k' is defined as

$$\begin{aligned} \xi_{\Delta k, \Delta l}^{k'} &\triangleq \frac{1}{2} \sum_{m=-\infty}^{\infty} f_{k,l}[m] f_{k',l'}^*[m] \\ &= \frac{1}{2} \left\{ \sum_{m=-\infty}^{\infty} f \left[m - \Delta k \frac{L}{2} \right] f[m] e^{-j2\pi \Delta l m/L} \right\} e^{-j\pi \Delta l k'}. \end{aligned} \quad (10)$$

According to (9), $\xi_{\Delta k, \Delta l}^{k'}$ indicates the interference proportion of $d_{k,l}$ on the desired symbol $d_{k',l'}$. On the other hand, since the prototype filter $f[m]$ has a compact pulse shape in time and frequency domains, the most power of interference on the desired symbol comes from the symbols at its time-frequency vicinity and the intruding effect of the other symbols can be considered trivial.^{10,24} Therefore, $y_{k',l'}$, presented in (9), becomes

$$y_{k',l'} = \sum_{\Delta k=-Q}^Q \sum_{\Delta l=-P}^P \xi_{\Delta k, \Delta l}^{k'} d_{k'-\Delta k, l'-\Delta l} + \omega_{k',l'}, \quad (11)$$

where Q and P are the maximum extension of $\xi_{\Delta k, \Delta l}^{k'}$ in time and frequency domains, respectively (ie, either $|\Delta k| > Q$ or $|\Delta l| > P$ leads to $\xi_{\Delta k, \Delta l}^{k'} \simeq 0$).

After presenting the FBMC/QAM interfering procedure with $\xi_{\Delta k, \Delta l}^{k'}$ at the next step, we demonstrate that $\xi_{\Delta k, \Delta l}^{k'}$ is inherently periodic through the frequency axis (ie, Δl); furthermore, we show that it can be periodic through the time axis (ie, Δk) by adding some redundant cyclic prefix (CP) and cyclic suffix (CS) to the transmitted symbol block.

3.1 | Periodicity of FBMC/QAM interference through the frequency axis

Since the number of subchannels of the FBMC/QAM (ie, L) is considered to be dividable by 2, from (10), we can derive that

$$\xi_{\Delta k, \Delta l \pm L}^{k'} = \xi_{\Delta k, \Delta l}^{k'}. \quad (12)$$

Equation 12 illustrates that $\xi_{\Delta k, \Delta l}^{k'}$ is periodic through the frequency axis with period L . By using this property, from (11), the demodulated symbols of all subchannels at time instance k' can be written in a matrix form as

$$\bar{y}_{k'} = \sum_{\Delta k=-Q}^Q \Psi_{\Delta k}^{k'} \bar{d}_{k'-\Delta k} + \bar{\omega}_{k'}, \quad (13)$$

where $\bar{y}_{k'} \triangleq [y_{k',0}, \dots, y_{k',L-1}]^T$, $\bar{d}_k \triangleq [d_{k,0}, \dots, d_{k,L-1}]^T$, and $\bar{\omega}_{k'} \triangleq [\omega_{k',0}, \dots, \omega_{k',L-1}]^T$. In (13), $\Psi_{\Delta k}^{k'}$ is a square matrix of the size $L \times L$, containing the $\xi_{\Delta k, \Delta l}^{k'}$ coefficients and, because of the periodicity of $\xi_{\Delta k, \Delta l}^{k'}$ (presented in Equation 12), is obtained as (14).

$$\Psi_{\Delta k}^{k'} = \begin{bmatrix} \xi_{\Delta k,0}^{k'} & \cdots & \xi_{\Delta k,-P+1}^{k'} & \xi_{\Delta k,-P}^{k'} & 0 & \cdots & 0 & 0 & \xi_{\Delta k,P}^{k'} & \cdots & \xi_{\Delta k,1}^{k'} \\ \vdots & \ddots & \vdots & \vdots & \vdots & \ddots & \vdots & \vdots & \vdots & \ddots & \vdots \\ \xi_{\Delta k,P-1}^{k'} & \cdots & \xi_{\Delta k,0}^{k'} & \cdots & \xi_{\Delta k,-P+1}^{k'} & \xi_{\Delta k,-P}^{k'} & 0 & 0 & 0 & 0 & \xi_{\Delta k,P}^{k'} \\ \xi_{\Delta k,P}^{k'} & \xi_{\Delta k,P-1}^{k'} & \cdots & \xi_{\Delta k,0}^{k'} & \cdots & \xi_{\Delta k,-P+1}^{k'} & \xi_{\Delta k,-P}^{k'} & 0 & \cdots & 0 & 0 \\ 0 & \xi_{\Delta k,P}^{k'} & \xi_{\Delta k,P-1}^{k'} & \cdots & \xi_{\Delta k,0}^{k'} & \cdots & \xi_{\Delta k,-P+1}^{k'} & \xi_{\Delta k,-P}^{k'} & 0 & \cdots & 0 \\ \vdots & \vdots & \vdots & \ddots & \vdots & \vdots & \vdots & \vdots & \vdots & \ddots & \vdots \\ 0 & \cdots & 0 & \xi_{\Delta k,P}^{k'} & \xi_{\Delta k,P-1}^{k'} & \cdots & \xi_{\Delta k,0}^{k'} & \cdots & \xi_{\Delta k,-P+1}^{k'} & \xi_{\Delta k,-P}^{k'} & 0 \\ 0 & 0 & \cdots & 0 & \xi_{\Delta k,P}^{k'} & \xi_{\Delta k,P-1}^{k'} & \cdots & \xi_{\Delta k,0}^{k'} & \cdots & \xi_{\Delta k,-P+1}^{k'} & \xi_{\Delta k,-P}^{k'} \\ \xi_{\Delta k,-P}^{k'} & 0 & 0 & \cdots & 0 & \xi_{\Delta k,P}^{k'} & \xi_{\Delta k,P-1}^{k'} & \cdots & \xi_{\Delta k,0}^{k'} & \cdots & \xi_{\Delta k,-P+1}^{k'} \\ \vdots & \vdots & \vdots & \ddots & \vdots & \vdots & \vdots & \ddots & \vdots & \vdots & \vdots \\ \xi_{\Delta k,-1}^{k'} & \cdots & \xi_{\Delta k,-P}^{k'} & 0 & 0 & \cdots & 0 & \xi_{\Delta k,P}^{k'} & \xi_{\Delta k,P-1}^{k'} & \cdots & \xi_{\Delta k,0}^{k'} \end{bmatrix}. \quad (14)$$

Note that $\Psi_{\Delta k}^{k'}$ is a circulant matrix, in which all rows and columns are constructed with the circular shifts of $\xi_{\Delta k,\Delta l}^{k'}$ coefficients for $\Delta l = -P, \dots, P$. Moreover, by using (10), it can be shown that $\xi_{\Delta k,\Delta l}^{k'+2} = \xi_{\Delta k,\Delta l}^{k'}$, which leads to $\Psi_{\Delta k}^{k'+2} = \Psi_{\Delta k}^{k'}$. Thus, for more facility, in the rest of this paper, we present $\xi_{\Delta k,\Delta l}^{k'}$ with $\xi_{\Delta k,\Delta l}^{+}$ and $\Psi_{\Delta k}^{k'}$ with $\Psi_{\Delta k}^{+}$ when k' is an even number and present $\xi_{\Delta k,\Delta l}^{k'}$ with $\xi_{\Delta k,\Delta l}^{-}$ and $\Psi_{\Delta k}^{k'}$ with $\Psi_{\Delta k}^{-}$ when k' is an odd number. Therefore, (13) can be rewritten as

$$\bar{y}_{k'} = \begin{cases} \sum_{\Delta k=-Q}^Q \Psi_{\Delta k}^{+} \bar{d}_{k'-\Delta k} + \bar{\omega}_{k'}; & \text{when } k' \text{ is even,} \\ \sum_{\Delta k=-Q}^Q \Psi_{\Delta k}^{-} \bar{d}_{k'-\Delta k} + \bar{\omega}_{k'}; & \text{when } k' \text{ is odd.} \end{cases} \quad (15)$$

3.2 | Periodicity of FBMC/QAM interference through the time axis

In the following, to make a periodicity through the time axis, suppose that the transmitter appends a CP and a CS, each with the length of Q , to the transmitted symbol block. In other words, we suppose that in a symbol block with length M time instances ($k = 0, \dots, M-1$, where $M > 2Q+1$), the first and last symbols of this block are organized as

$$\begin{aligned} \bar{d}_k &= \bar{d}_{k+M-2Q}; & \text{for } k = 0, \dots, Q-1, \\ \bar{d}_k &= \bar{d}_{k-M+2Q}; & \text{for } k = M-Q, \dots, M-1. \end{aligned} \quad (16)$$

Figure 1 illustrates the principle of appending CP and a CS to the symbol block. At the receiver, after removing the CP (for $k = 0, \dots, Q-1$) and CS (for $k = M-Q, \dots, M-1$), the remaining symbol block has the circulant property, regarding the time axis, such that by defining $\bar{y} = [\bar{y}_Q^T, \dots, \bar{y}_{M-Q-1}^T]^T$, $\bar{d} = [\bar{d}_Q^T, \dots, \bar{d}_{M-Q-1}^T]^T$, and $\bar{\omega} = [\bar{\omega}_Q^T, \dots, \bar{\omega}_{M-Q-1}^T]^T$, according to (15), the demodulated symbols at each symbol block can be presented in a matrix form as

$$\bar{y} = \mathbf{Z}\bar{d} + \bar{\omega}, \quad (17)$$

where \mathbf{Z} is a square matrix of the size $LN \times LN$ (note that $N \stackrel{\Delta}{=} M-2Q$), which by assuming that N and Q are even numbers, it can be presented as (18). According to (17), \mathbf{Z} can be interpreted as the transmission matrix of the FBMC/QAM system.

$$\mathbf{Z} = \begin{bmatrix} \Psi_0^{+} & \cdots & \Psi_{-Q+1}^{+} & \Psi_{-Q}^{+} & 0 & \cdots & 0 & 0 & \Psi_Q^{+} & \cdots & \Psi_1^{+} \\ \vdots & \ddots & \vdots & \vdots & \vdots & \ddots & \vdots & \vdots & \vdots & \ddots & \vdots \\ \Psi_{Q-1}^{-} & \cdots & \Psi_0^{-} & \cdots & \Psi_{-Q+1}^{-} & \Psi_{-Q}^{-} & 0 & 0 & 0 & 0 & \Psi_Q^{-} \\ \Psi_Q^{+} & \Psi_{Q-1}^{+} & \cdots & \Psi_0^{+} & \cdots & \Psi_{-Q+1}^{+} & \Psi_{-Q}^{+} & 0 & \cdots & 0 & 0 \\ 0 & \Psi_Q^{-} & \Psi_{Q-1}^{-} & \cdots & \Psi_0^{-} & \cdots & \Psi_{-Q+1}^{-} & \Psi_{-Q}^{-} & 0 & \cdots & 0 \\ \vdots & \vdots & \vdots & \ddots & \vdots & \vdots & \vdots & \vdots & \vdots & \ddots & \vdots \\ 0 & \cdots & 0 & \Psi_Q^{+} & \Psi_{Q-1}^{+} & \cdots & \Psi_0^{+} & \cdots & \Psi_{-Q+1}^{+} & \Psi_{-Q}^{+} & 0 \\ 0 & 0 & \cdots & 0 & \Psi_Q^{-} & \Psi_{Q-1}^{-} & \cdots & \Psi_0^{-} & \cdots & \Psi_{-Q+1}^{-} & \Psi_{-Q}^{-} \\ \Psi_{-Q}^{+} & 0 & 0 & \cdots & 0 & \Psi_Q^{+} & \Psi_{Q-1}^{+} & \cdots & \Psi_0^{+} & \cdots & \Psi_{-Q+1}^{+} \\ \vdots & \vdots & \vdots & \ddots & \vdots & \vdots & \vdots & \ddots & \vdots & \vdots & \vdots \\ \Psi_{-1}^{-} & \cdots & \Psi_{-Q}^{-} & 0 & 0 & \cdots & 0 & \Psi_Q^{-} & \Psi_{Q-1}^{-} & \cdots & \Psi_0^{-} \end{bmatrix}. \quad (18)$$

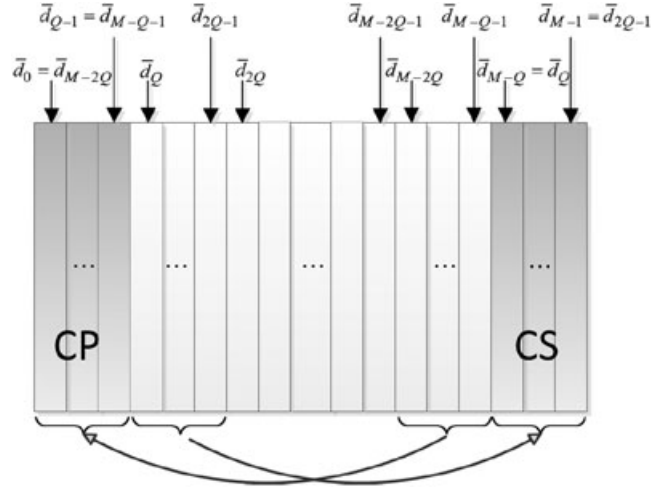


FIGURE 1 Principle of appending cyclic prefix (CP) and cyclic suffix (CS), with length of Q , into the transmitted block with length M

$$\mathbf{A} = \begin{bmatrix} \mathbf{B}_0 & \cdots & \mathbf{B}_{-\eta+1} & \mathbf{B}_{-\eta} & \mathbf{0} & \cdots & \mathbf{0} & \mathbf{0} & \mathbf{B}_\eta & \cdots & \mathbf{B}_1 \\ \vdots & \ddots & \vdots & \vdots & \vdots & \ddots & \vdots & \vdots & \vdots & \ddots & \vdots \\ \mathbf{B}_{\eta-1} & \cdots & \mathbf{B}_0 & \cdots & \mathbf{B}_{-\eta+1} & \mathbf{B}_{-\eta} & \mathbf{0} & \mathbf{0} & \mathbf{0} & \cdots & \mathbf{B}_\eta \\ \mathbf{B}_\eta & \mathbf{B}_{\eta-1} & \cdots & \mathbf{B}_0 & \cdots & \mathbf{B}_{-\eta+1} & \mathbf{B}_{-\eta} & \mathbf{0} & \cdots & \mathbf{0} & \mathbf{0} \\ \mathbf{0} & \mathbf{B}_\eta & \mathbf{B}_{\eta-1} & \cdots & \mathbf{B}_0 & \cdots & \mathbf{B}_{-\eta+1} & \mathbf{B}_{-\eta} & \mathbf{0} & \cdots & \mathbf{0} \\ \vdots & \vdots & \vdots & \ddots & \vdots & \vdots & \vdots & \vdots & \vdots & \ddots & \vdots \\ \mathbf{0} & \cdots & \mathbf{0} & \mathbf{B}_\eta & \mathbf{B}_{\eta-1} & \cdots & \mathbf{B}_0 & \cdots & \mathbf{B}_{-\eta+1} & \mathbf{B}_{-\eta} & \mathbf{0} \\ \mathbf{0} & \mathbf{0} & \cdots & \mathbf{0} & \mathbf{B}_\eta & \mathbf{B}_{\eta-1} & \cdots & \mathbf{B}_0 & \cdots & \mathbf{B}_{-\eta+1} & \mathbf{B}_{-\eta} \\ \mathbf{B}_{-\eta} & \mathbf{0} & \mathbf{0} & \cdots & \mathbf{0} & \mathbf{B}_\eta & \mathbf{B}_{\eta-1} & \cdots & \mathbf{B}_0 & \cdots & \mathbf{B}_{-\eta+1} \\ \vdots & \vdots & \vdots & \ddots & \vdots & \vdots & \vdots & \vdots & \vdots & \ddots & \vdots \\ \mathbf{B}_{-1} & \cdots & \mathbf{B}_{-\eta} & \mathbf{0} & \mathbf{0} & \cdots & \mathbf{0} & \mathbf{B}_\eta & \mathbf{B}_{\eta-1} & \cdots & \mathbf{B}_0 \end{bmatrix}. \quad (19)$$

To investigate the time-frequency symbol density of FBMC/QAM, in the next section, we determine the rank of the transmission matrix \mathbf{Z} .

3.3 | Rank of the FBMC/QAM transmission matrix

To obtain the maximal symbol density that can be supported by FBMC/QAM, the rank of the transmission matrix \mathbf{Z} is determinative. To specify the rank of \mathbf{Z} , its eigenvalues need to be calculated. In this regard, for more facility, let us define the circulant function $\mathbf{A} = \text{circ}(\mathbf{B}, \beta)$, in which β is a positive number and \mathbf{B} is a matrix defined as $\mathbf{B} \triangleq [\mathbf{B}_{-\eta}, \dots, \mathbf{B}_0, \dots, \mathbf{B}_\eta]$. Each submatrix \mathbf{B}_i , for $i = -\eta, \dots, \eta$, is a square matrix of the size $\alpha \times \alpha$. Thus, when $\beta > 2\eta + 1$, the circulant function returns the matrix \mathbf{A} of the size $\alpha\beta \times \alpha\beta$ as (19). As a result, the circulant matrix $\Psi_{\Delta k}^{k'}$ in (14) can be represented with the circulant function as

$$\Psi_{\Delta k}^{k'} = \text{circ}([\xi_{\Delta k, -P}^{k'}, \dots, \xi_{\Delta k, 0}^{k'}, \dots, \xi_{\Delta k, P}^{k'}], L). \quad (20)$$

Also, it can be easily shown that matrix \mathbf{Z} in (18) can be illustrated with the circulant function as

$$\mathbf{Z} = \text{circ}([\Theta_{-Q/2}, \dots, \Theta_0, \dots, \Theta_{Q/2}], N/2), \quad (21)$$

in which Θ_i , for $i = -Q/2, \dots, Q/2$, is a $2L \times 2L$ matrix defined as

$$\Theta_i \triangleq \begin{bmatrix} \Psi_{2i}^+ & \Psi_{2i-1}^+ \\ \Psi_{2i+1}^- & \Psi_{2i}^- \end{bmatrix}. \quad (22)$$

In addition, before deriving the eigenvalues of \mathbf{Z} , we need to mention 3 lemmas as follows:

Lemma 1. Assume that matrix Ψ is a circulant matrix of the size $\beta \times \beta$, which can be presented as

$$\Psi = \text{circ}([a_{-\eta}, \dots, a_0, \dots, a_\eta], \beta). \quad (23)$$

Also, assume that \mathbf{F}_β is the discrete Fourier transform matrix of the size $\beta \times \beta$. In this case, matrix $\mathbf{V} \triangleq \mathbf{F}_\beta^H \mathbf{\Psi} \mathbf{F}_\beta$ will be a diagonal matrix, and the entries of its diagonal are the β -point inverse discrete Fourier transform of a_i for $i = -\eta, \dots, \eta$.²¹ In other words, the (p, p) th entry of \mathbf{V} is

$$(\mathbf{V})_{p,p} = \sum_{i=0}^{\beta-1} a_{[i]_\beta} e^{j2\pi ip/\beta}, \quad (24)$$

where $[.]_\beta$ is the modulo operator.

Lemma 2. Assume that the circulant matrix \mathbf{T} of the size $\beta \times \beta$ is defined as

$$\mathbf{T} = \text{circ}([\Phi_{-\eta}, \dots, \Phi_0, \dots, \Phi_\eta], \beta/2), \quad (25)$$

in which for $i = -\eta, \dots, \eta$, Φ_i is a 2×2 matrix constructed with a_i, b_i, c_i , and d_i such that

$$\Phi_i = \begin{bmatrix} a_i & d_i \\ c_i & b_i \end{bmatrix}. \quad (26)$$

Also, suppose that $\Lambda \triangleq \mathbf{F}_\beta^H \mathbf{T} \mathbf{F}_\beta$. Then, the (n, q) th entry of Λ , for $n, q = 0, \dots, \beta - 1$ is

$$(\Lambda)_{n,q} = \begin{cases} \frac{1}{2} \begin{pmatrix} a'_n + b'_n + e^{j2\pi n/N} c'_n \\ + e^{-j2\pi n/N} d'_n \end{pmatrix} & ; \text{if } n = q, \\ \frac{1}{2} \begin{pmatrix} a'_n - b'_n + e^{j2\pi n/N} c'_n \\ - e^{-j2\pi n/N} d'_n \end{pmatrix} & ; \text{if } n = q \pm N/2, \\ 0 & ; \text{otherwise,} \end{cases} \quad (27)$$

where a'_n, b'_n, c'_n , and d'_n , for $n = 0, \dots, \beta - 1$, are defined as

$$\begin{aligned} a'_n &= \sum_{i=0}^{\beta/2-1} a_{[i]_{\beta/2}} e^{j2\pi in/(\beta/2)}, \\ b'_n &= \sum_{i=0}^{\beta/2-1} b_{[i]_{\beta/2}} e^{j2\pi in/(\beta/2)}, \\ c'_n &= \sum_{i=0}^{\beta/2-1} c_{[i]_{\beta/2}} e^{j2\pi in/(\beta/2)}, \\ d'_n &= \sum_{i=0}^{\beta/2-1} d_{[i]_{\beta/2}} e^{j2\pi in/(\beta/2)}. \end{aligned} \quad (28)$$

Proof. See Appendix A. □

Lemma 3. Assume that Λ is a matrix of the size 2×2 , presented as

$$\Lambda = \begin{bmatrix} r_{0,0} & r_{0,1} \\ r_{0,1}^* & r_{1,1} \end{bmatrix}, \quad (29)$$

in which $r_{0,0}$ and $r_{1,1}$ are real and $r_{0,1}$ is complex. If the diagonal matrix Σ contains the eigenvalues of Λ , then it can be presented as

$$\Sigma = \begin{bmatrix} \varepsilon_0 & 0 \\ 0 & \varepsilon_1 \end{bmatrix}, \quad (30)$$

in which ε_0 and ε_1 are calculated as

$$\begin{aligned} \varepsilon_0 &= \frac{1}{2} \left(\frac{r_{0,0} + r_{1,1}}{+\sqrt{[r_{0,0} - r_{1,1}]^2 + 4|r_{0,1}|^2}} \right), \\ \varepsilon_1 &= \frac{1}{2} \left(\frac{r_{0,0} + r_{1,1}}{-\sqrt{[r_{0,0} - r_{1,1}]^2 + 4|r_{0,1}|^2}} \right). \end{aligned} \quad (31)$$

By using these 3 mentioned lemmas, we will determine the rank of the FBMC/QAM transmission matrix by proving the following theorem:

Theorem 1. *The rank of the $LN \times LN$ matrix \mathbf{Z} , presented in (21), is $LN/2$ such that the half of eigenvalues of this matrix are exactly ones and other half of eigenvalues are zeros.*

Proof. We illustrated that \mathbf{Z} , appeared in (17), can be presented with the circulant function. The calculation of the eigenvalues of \mathbf{Z} in this form is very difficult. Thus, to simplify the process, we define the matrix \mathbf{T} , which its eigenvalues are equivalent to those of \mathbf{Z} such that

$$\mathbf{T} \stackrel{\Delta}{=} \mathbf{X}^H \mathbf{Z} \mathbf{X}, \quad (32)$$

where \mathbf{X} is a unitary matrix of the size $NL \times NL$ and is defined as

$$\mathbf{X} \stackrel{\Delta}{=} \text{kron}(\mathbf{I}_N, \mathbf{F}_L). \quad (33)$$

Since \mathbf{X} is a unitary matrix, the eigenvalues of \mathbf{Z} and \mathbf{T} are the same²²; thus, we can find the eigenvalues of \mathbf{T} , instead of \mathbf{Z} . Substituting the presentation of (21) and (22) into (32) and considering (33), it is concluded that \mathbf{T} can be written as

$$\mathbf{T} = \text{circ}([\Phi_{-Q/2}, \dots, \Phi_0, \dots, \Phi_{Q/2}], N/2), \quad (34)$$

in which Φ_i , for $i = -Q/2, \dots, Q/2$, is a $2L \times 2L$ matrix defined as

$$\Phi_i = \begin{bmatrix} \mathbf{F}_L^H \Psi_{2i}^+ \mathbf{F}_L & \mathbf{F}_L^H \Psi_{2i-1}^+ \mathbf{F}_L \\ \mathbf{F}_L^H \Psi_{2i+1}^- \mathbf{F}_L & \mathbf{F}_L^H \Psi_{2i}^- \mathbf{F}_L \end{bmatrix}. \quad (35)$$

Since Ψ_{i+} and Ψ_{i-} for $i = -Q \dots, Q$ are circulant matrixes (see Equation 14), according to Lemma 1, $\mathbf{V}_{2i}^+ \stackrel{\Delta}{=} \mathbf{F}_L^H \Psi_{2i}^+ \mathbf{F}_L$, $\mathbf{V}_{2i}^- \stackrel{\Delta}{=} \mathbf{F}_L^H \Psi_{2i}^- \mathbf{F}_L$, $\mathbf{V}_{2i+1}^- \stackrel{\Delta}{=} \mathbf{F}_L^H \Psi_{2i+1}^- \mathbf{F}_L$, and $\mathbf{V}_{2i-1}^+ \stackrel{\Delta}{=} \mathbf{F}_L^H \Psi_{2i-1}^+ \mathbf{F}_L$ all become diagonal matrixes of the size $L \times L$, which their (p, p) th entries are

$$\begin{aligned} (\mathbf{V}_{2i}^+)_{p,p} &= \sum_{\Delta l=0}^{L-1} \xi_{2i, [\Delta l]_L}^+ e^{j2\pi \Delta l p/L}, \\ (\mathbf{V}_{2i}^-)_{p,p} &= \sum_{\Delta l=0}^{L-1} \xi_{2i, [\Delta l]_L}^- e^{j2\pi \Delta l p/L}, \\ (\mathbf{V}_{2i+1}^-)_{p,p} &= \sum_{\Delta l=0}^{L-1} \xi_{2i+1, [\Delta l]_L}^- e^{j2\pi \Delta l p/L}, \\ (\mathbf{V}_{2i-1}^+)_{p,p} &= \sum_{\Delta l=0}^{L-1} \xi_{2i-1, [\Delta l]_L}^+ e^{j2\pi \Delta l p/L}. \end{aligned} \quad (36)$$

□

On the other hand, matrix \mathbf{T} in (34) corresponds to the condition of Lemma 2; thus, let us define

$$\mathbf{\Lambda} = \mathbf{E}^H \mathbf{T} \mathbf{E}, \quad (37)$$

where $\mathbf{E} \stackrel{\Delta}{=} \text{kron}(\mathbf{F}_N, \mathbf{I}_L)$. Note that, since \mathbf{E} is a unitary matrix, the eigenvalues of $\mathbf{\Lambda}$ are equivalent to those of \mathbf{T} (and also those of \mathbf{Z}); then, we will calculate the eigenvalues of $\mathbf{\Lambda}$. According to Lemma 2, $\mathbf{\Lambda}^{(n,q)}$ (ie, the (n, q) th submatrix of $\mathbf{\Lambda}$ of the size $L \times L$) is a diagonal matrix, which is obtained as

$$\mathbf{\Lambda}^{(n,q)} = \begin{cases} \frac{1}{2} (\mathbf{A}'_n + \mathbf{B}'_n + e^{j2\pi n/N} \mathbf{C}'_n + e^{-j2\pi n/N} \mathbf{D}'_n) & ; \text{if } n = q, \\ \frac{1}{2} (\mathbf{A}'_n - \mathbf{B}'_n + e^{j2\pi n/N} \mathbf{C}'_n - e^{-j2\pi n/N} \mathbf{D}'_n) & ; \text{if } n = q \pm N/2, \\ \mathbf{0}_L & ; \text{otherwise,} \end{cases} \quad (38)$$

where \mathbf{A}'_n , \mathbf{B}'_n , \mathbf{C}'_n , and \mathbf{D}'_n , for $n = 0, \dots, N-1$, are diagonal matrixes such that

$$\begin{aligned}\mathbf{A}'_n &= \sum_{i=0}^{N/2-1} \mathbf{V}_{[2i]_{N/2}}^+ e^{j2\pi in/(N/2)}, \\ \mathbf{B}'_n &= \sum_{i=0}^{N/2-1} \mathbf{V}_{[2i]_{N/2}}^- e^{j2\pi in/(N/2)}, \\ \mathbf{C}'_n &= \sum_{i=0}^{N/2-1} \mathbf{V}_{[2i+1]_{N/2}}^- e^{j2\pi in/(N/2)}, \\ \mathbf{D}'_n &= \sum_{i=0}^{N/2-1} \mathbf{V}_{[2i-1]_{N/2}}^+ e^{j2\pi in/(N/2)}.\end{aligned}\quad (39)$$

Substituting (36) into (39), the (p, p) th entry of \mathbf{A}'_n , \mathbf{B}'_n , \mathbf{C}'_n , and \mathbf{D}'_n becomes

$$\begin{aligned}(\mathbf{A}'_n)_{p,p} &= \sum_{i=0}^{N/2-1} \sum_{\Delta l=0}^{L-1} \xi_{[2i]_{N/2}, [\Delta l]_L}^+ e^{j2\pi \Delta l p/L} e^{j2\pi in/(N/2)}, \\ (\mathbf{B}'_n)_{p,p} &= \sum_{i=0}^{N/2-1} \sum_{\Delta l=0}^{L-1} \xi_{[2i]_{N/2}, [\Delta l]_L}^- e^{j2\pi \Delta l p/L} e^{j2\pi in/(N/2)}, \\ (\mathbf{C}'_n)_{p,p} &= \sum_{i=0}^{N/2-1} \sum_{\Delta l=0}^{L-1} \xi_{[2i+1]_{N/2}, [\Delta l]_L}^- e^{j2\pi \Delta l p/L} e^{j2\pi in/(N/2)}, \\ (\mathbf{D}'_n)_{p,p} &= \sum_{i=0}^{N/2-1} \sum_{\Delta l=0}^{L-1} \xi_{[2i-1]_{N/2}, [\Delta l]_L}^+ e^{j2\pi \Delta l p/L} e^{j2\pi in/(N/2)}.\end{aligned}\quad (40)$$

On the other hand, note that, from (10), it is resulted that when Δk is an even number, $\xi_{\Delta k, \Delta l-} = (-1)^{\Delta l} \xi_{\Delta k, \Delta l+}$; also, when Δk is an odd number, $\xi_{\Delta k, \Delta l-} = \xi_{-\Delta k, \Delta l+}$; thus, (40) can be all rewritten in terms of $\xi_{\Delta k, \Delta l+}$, such that

$$\begin{aligned}(\mathbf{A}'_n)_{p,p} &= \sum_{i=0}^{N/2-1} \sum_{\Delta l=0}^{L-1} \xi_{[2i]_{N/2}, [\Delta l]_L}^+ e^{j2\pi \Delta l p/L} e^{j2\pi in/(N/2)}, \\ (\mathbf{B}'_n)_{p,p} &= \sum_{i=0}^{N/2-1} \sum_{\Delta l=0}^{L-1} (-1)^{\Delta l} \xi_{[2i]_{N/2}, [\Delta l]_L}^+ e^{j2\pi \Delta l p/L} e^{j2\pi in/(N/2)}, \\ (\mathbf{C}'_n)_{p,p} &= \sum_{i=0}^{N/2-1} \sum_{\Delta l=0}^{L-1} \xi_{[-2i-1]_{N/2}, [\Delta l]_L}^+ e^{j2\pi \Delta l p/L} e^{j2\pi in/(N/2)}, \\ (\mathbf{D}'_n)_{p,p} &= \sum_{i=0}^{N/2-1} \sum_{\Delta l=0}^{L-1} \xi_{[2i-1]_{N/2}, [\Delta l]_L}^+ e^{j2\pi \Delta l p/L} e^{j2\pi in/(N/2)}.\end{aligned}\quad (41)$$

As is clear from (41), $(\mathbf{D}'_n)_{p,p} = (\mathbf{C}'_n)_{p,p}^*$; as a result, (38) can be simplified to

$$\Lambda^{(n,q)} = \begin{cases} \frac{1}{2} (\mathbf{A}'_n + \mathbf{B}'_n + 2\text{Re}\{e^{j2\pi n/N} \mathbf{C}'_n\}) & ; \text{if } n = q, \\ \frac{1}{2} (\mathbf{A}'_n - \mathbf{B}'_n + j2\text{Im}\{e^{j2\pi n/N} \mathbf{C}'_n\}) & ; \text{if } n = q \pm N/2, \\ \mathbf{0}_L & ; \text{otherwise.} \end{cases}\quad (42)$$

Furthermore, we show in Appendix B that, for a prototype pulse shape, satisfying the condition (2), we have always

$$\begin{aligned}\mathbf{A}'_n + \mathbf{B}'_n &= \mathbf{I}_L, \\ \mathbf{A}'_n - \mathbf{B}'_n &= \mathbf{0}_L, \\ |\mathbf{C}'_n| &= \frac{1}{2} \mathbf{I}_L.\end{aligned}\quad (43)$$

Substituting the first 2 terms of (43) into (42) leads to

$$\Lambda^{(n,q)} = \begin{cases} \frac{1}{2}[\mathbf{I}_L + 2\text{Re}\{e^{j2\pi n/N} \mathbf{C}'_n\}] & ; \text{ if } n = q, \\ j\text{Im}\{e^{j2\pi n/N} \mathbf{C}'_n\} & ; \text{ if } n = q \pm N/2, \\ \mathbf{0}_L & ; \text{ otherwise.} \end{cases} \quad (44)$$

According to (44), matrix Λ can be represented in the form of

$$\Lambda = \begin{bmatrix} \mathbf{R}^{(0,0)} & \mathbf{R}^{(0,1)} \\ \mathbf{R}^{(0,1)*} & \mathbf{R}^{(1,1)} \end{bmatrix}, \quad (45)$$

in which $\mathbf{R}^{(0,0)}$ and $\mathbf{R}^{(1,1)}$ are real-valued diagonal matrixes and $\mathbf{R}^{(0,1)}$ is a complex diagonal matrix. Note that, $\mathbf{R}^{(0,0)}$, $\mathbf{R}^{(1,1)}$, and $\mathbf{R}^{(0,1)}$, of the size $NL/2 \times NL/2$, are defined as

$$\begin{aligned} \mathbf{R}^{(0,0)} &\triangleq \begin{bmatrix} \frac{1}{2}\mathbf{I}_L + \text{Re}\{e^{j2\pi 0/N} \mathbf{C}'_0\} & & \mathbf{0} \\ & \ddots & \\ \mathbf{0} & & \frac{1}{2}\mathbf{I}_L + \text{Re}\{e^{j2\pi(N/2-1)/N} \mathbf{C}'_{N/2-1}\} \end{bmatrix}, \\ \mathbf{R}^{(0,1)} &\triangleq \begin{bmatrix} j\text{Im}\{e^{j2\pi 0/N} \mathbf{C}'_n\} & & \mathbf{0} \\ & \ddots & \\ \mathbf{0} & & j\text{Im}\{e^{j2\pi(N/2-1)/N} \mathbf{C}'_{N/2-1}\} \end{bmatrix}, \\ \mathbf{R}^{(1,1)} &\triangleq \begin{bmatrix} \frac{1}{2}\mathbf{I}_L - \text{Re}\{e^{j2\pi 0/N} \mathbf{C}'_0\} & & \mathbf{0} \\ & \ddots & \\ \mathbf{0} & & \frac{1}{2}\mathbf{I}_L - \text{Re}\{e^{j2\pi(N/2-1)/N} \mathbf{C}'_{N/2-1}\} \end{bmatrix}. \end{aligned} \quad (46)$$

From (45), it is obvious that Λ matches the condition of Lemma 3; thus, by considering (46) and the last term of (43), into (31), the diagonal matrix Σ containing all eigenvalues of Λ becomes

$$\Sigma = \begin{bmatrix} \mathbf{I}_{NL/2} & \mathbf{0}_{NL/2} \\ \mathbf{0}_{NL/2} & \mathbf{0}_{NL/2} \end{bmatrix}. \quad (47)$$

As (47) illustrates, the half eigenvalues of Λ are exactly ones and the other half are zeros. Also, according to (32) and (37), $\Lambda = (\mathbf{X}\mathbf{E})^H \mathbf{Z}\mathbf{X}\mathbf{E}$; since \mathbf{X} and \mathbf{E} are unitary matrixes, the eigenvalues of Λ and \mathbf{Z} are equivalent; thus, it is concluded that the half eigenvalues of \mathbf{Z} are ones and the other half are zeros; as a result, the rank of \mathbf{Z} , with the size of $NL \times NL$, is $NL/2$ and the theorem is proved.

4 | TIME-FREQUENCY SYMBOL DENSITY OF FBMC/QAM

In the previous section, we showed that the FBMC/QAM system with CP and CS has a rank-deficient transmission matrix, such that the half of its eigenvalues are exactly 1 and the other half is 0. In this regard and also considering (17), since the number of equations should be at least equal to the number of unknowns, one can conclude that the transmitted vector, \vec{d} , of the size $LN \times 1$ must be linearly constructed from maximum $LN/2$ independent QAM symbol, such that

$$\vec{d} = \mathbf{G}\vec{u}, \quad (48)$$

where \mathbf{G} is the precoding matrix of the size $LN \times (LN/2)$ and \vec{u} is the QAM symbol vector of the size $(LN/2) \times 1$. Accordingly, the FBMC/QAM time-frequency symbol density can be calculated as

$$D = \frac{NL/2}{(MN_0)(LF_0)} = \frac{N}{N + 2Q}. \quad (49)$$

From (49), it is concluded that the quantity of the symbol density of FBMC/QAM, D , just depends on N (the length of symbol block for which a CP and a CS is appended) and $2Q$ (the total extension of the prototype filter through the time). It must be noted that, since the interference of FBMC/QAM is inherently circulant regarding the frequency axis, the extension of the prototype filter through the frequency does not affect the symbol density.

On the other hand, looking for the maximal symbol density, we suppose that $N \rightarrow \infty$, which leads to $D = 1$. This symbol density is exactly equivalent to that of the primer OFDM/OQAM. In other words, one can say that, in addition to

handling the SM techniques in MIMO channels, FBMC/QAM system has the potential to provide the maximum achievable bandwidth efficiency for a multicarrier system.

5 | RELATED WORKS

Recently, some limited studies try to achieve the spatial diversity by adapting the complex SM techniques to the FBMC/QAM system.^{20,23-26} In these studies, the Alamouti coding, as the only orthogonal STBC, has been considered to achieve the maximum diversity gain. In Lin et al,²³ an FBMC/QAM pseudo-Alamouti scheme has been introduced, which requires a CP as a guard interval. The length of CP needs to be at least equal to the time dispersion of the channel and, as a result, this scheme suffers from the lack of spectral efficiency. Renfors et al²⁰ proposed a method, in which, instead of CP, a zero-padded gap is used to avoid the interference. Because of this gap, in this scheme, the lack of bandwidth efficiency is considerable.

In Lele et al,^{24,25} the code division multiple access is combined with the FBMC/QAM to transmit the complex symbols and the bandwidth efficiency of this system is related to the number of users of code division multiple access. Also, Zakaria and Le Ruyet²⁶ proposed a method titled as fast Fourier transform filter bank multicarrier, in which a CP OFDM technique is applied at each subcarrier of FBMC/QAM to eliminate the interference. In such a system, complex symbols are transmitted and SM techniques can be directly applied but the system suffers from the diminishing bandwidth efficiency because of using CP. In fast Fourier transform filter bank multicarrier, the length of CP is equal to the prototype filter's time dispersion.

To compare the achieved symbol density in the mentioned schemes to the maximal symbol density of an FBMC/QAM system derived in this article (ie, $D = 1$), consider an FBMC/QAM system in the situation presented in Table 1. In this regard, the obtained symbol density for the above schemes is summarized in Table 2. As is obvious from Table 2, the symbol densities of these methods are lower than the maximal density $D = 1$, which asserts this fact that the ultimate maximal symbol density of any FBMC/QAM scheme, with the ability of perfectly removing the interferences, is $D = 1$.

TABLE 1 FBMC/QAM parameters

Parameter	Value/Type
modulation	4-QAM
prototype filter	IOTA
sampling period	$t_s = 100$ ns
carrier frequency	$f_c = 2$ GHz
number of filter bank subchannels	$L = 128$
fading channel model	Vehicular-A
CP length	$\nu = 24$
number of users in CDMA based schemes	$U = 32$
FFT-FBMC per-subchannel-OFDM size	$\alpha = 32$
FFT-FBMC CP length	$\nu = 4$

Abbreviations: CDMA, code division multiple access; CP, cyclic prefix; FBMC, filter bank multicarrier; FFT, fast Fourier transform; OFDM, orthogonal frequency division multiplexing; QAM, quadrature amplitude modulation.


TABLE 2 The achieved symbol density by considering the situation of Table 1

Type of scheme	Achieved symbol density (D)
Proposed scheme in Lin et al ²³	0.84
Proposed scheme in Renfors et al ²⁰	0.84
Proposed schemes in Lele et al ^{24,25}	0.5
Proposed scheme in Zakaria and Le Ruyet ²⁶	0.89

6 | CONCLUSIONS

To achieve the full diversity gain of MIMO channels, the SM techniques are applicable to the FBMC/QAM schemes transmitting complex symbols, instead of real-valued ones. In this article, we firstly presented a matrix formulation for FBMC/QAM modulation. To achieve this purpose, we showed that the interference procedure is intrinsically periodic through the frequency axis, and also, it becomes periodic through the time axis by appending some CP and CS to the transmitted symbol block. On the basis of this matrix presentation, we showed that, in FBMC/QAM, the maximal achievable time-frequency symbol density, with the ability of perfectly removing the interferences, is exactly equal to that of the primer OFDM/OQAM.

ORCID

Seyyed Mohammad Javad Asgari Tabatabaee  <http://orcid.org/0000-0002-2712-4105>

REFERENCES

1. Gao J, Li J, Cai Z, Gao H. Composite event coverage in wireless sensor networks with heterogeneous sensors. In: Proceedings of 2015 IEEE Conference on Computer Communications (INFOCOM); 2015; Kowloon. 217-225.
2. Zhang Q, Yang LT, Chen Z, Li P, Deen MJ. Privacy-preserving double-projection deep computation model with crowdsourcing on cloud for big data feature learning. *IEEE Internet Things J.* 2017;(99):1-1.
3. Zhang Q, Yang LT, Liu X, Chen Z, Li P. A tucker deep computation model for mobile multimedia feature learning. *ACM Trans Multimed Comput Commun Appl (TOMM).* 2017;13(3s):39.
4. Li P, Chen Z, Yang LT, Zhang Q, Deen MJ. Deep convolutional computation model for feature learning on big data in internet of things. *IEEE Trans Ind Informat.* 2017;(99):1-1.
5. Gao J, Li J, Li Y. Approximate event detection over multi-modal sensing data. *J Comb Optim.* 2016;32(4):1002-1016.
6. Vakilian V, Wild T, Schaich F, ten Brink S, Frigon J-F. Universal-filtered multi-carrier technique for wireless systems beyond LTE. In: Proc. 9th Int. Workshop on Broadband Wireless Access, IEEE Global Commun. Conf. (Globecom13). Atlanta, GA, USA; 2013:223-228.
7. Wunder G, Jung P, Kasparick M. 5GNOW: non-orthogonal, asynchronous waveforms for future mobile applications. *IEEE Commun Mag.* 2014;52(2):97-105.
8. Gharba M, Legouable R, Siohan P. An alternative multiple access scheme for the uplink 3GPP/LTE based on OFDM/OQAM. In: Proc. IEEE Int. Symp. Wireless Commun. Syst. (ISWCS); 2010; York, England. 941-945.
9. Amini P, Rong-Rong C, Farhang-Boroujeny B. Filterbank multicarrier communications for underwater acoustic channels. *IEEE J Ocean Eng.* 2015;40(1):115-130.
10. Farhang-Boroujeny B. OFDM versus filter bank multicarrier. *IEEE Signal Process Mag.* 2011;28(3):92-112.
11. Sahin A, Guvenc I, Arslan H. A survey on multicarrier communications prototype filters, lattice structures, and implementation aspects. *IEEE Commun Surveys Tuts.* 2014;16(3):1312-1338.
12. Saltzberg BR. Performance of an efficient parallel data transmission system. *IEEE Trans Commun Technol.* 1967;15(6):805-811.
13. Farhang-Boroujeny B, Yuen C. Cosine modulated and offset QAM filter bank multicarrier techniques: a continuous-time prospect. *EURASIP J Adv Signal Process.* 2010;6:1-16.
14. Zhang H, Le Ruyet D, Roviras D, Medjahdi Y, Sun H. Spectral efficiency comparison of OFDM/FBMC for uplink cognitive radio networks. *EURASIP Journal on Advances in Signal Processing.* 2010;2010(1):1-14.
15. Asgari Tabatabaee SMJ, Zamiri-Jafarian H. Per-subchannel joint equalizer and receiver filter design in OFDM/OQAM systems. *IEEE Trans Signal Process;* 64(19):5094-5105.
16. Farhang-Boroujeny B, Schlegel C. Efficient multicarrier realization of full-rate space-time orthogonal block coded systems. In: International Conference on Communications, 2003. ICC'03 IEEE, Vol. 4; 2003:2267-2271.
17. Amini P, Chen RR, Farhang-Boroujeny B. Filterbank multicarrier communications for underwater acoustic channels. *IEEE J Ocean Eng;* 40(1):115-130.
18. Benedetto JJ, Heil C, Walnut DF. Gabor systems and the Balian-Low theorem. *Gabor Analysis and Algorithms.* Springer: Birkhuser Boston; 1998:85-122.
19. Ihalainen T, Hidalgo Stitz T, Rinne M, Renfors M. Channel equalization in filter-bank-based multicarrier modulation for wireless communications. *EURASIP J Adv Signal Process.* 2007;2007(1):1-18.
20. Renfors M, Ihalainen T, Stitz TH. A block-Alamouti scheme for filter bank based multicarrier transmission. In: Lucca, Italy; 1038-1041.
21. Goldsmith A. *Wireless Communications:* Cambridge University Press; 2005.
22. Golub G, Van Loan C. *Matrix Computations.* 3rd ed. Baltimore: Johns Hopkins University Press.
23. Lin H, Lele C, Siohan P. A pseudo Alamouti transceiver design for OFDM/OQAM modulation with cyclic prefix. In: IEEE Workshop on Signal Processing Advances in Wireless Communications (SPAWC 09); 2009; Perugia, Italy. 300-304.

24. Lele C, Sioha P, Legouable R, Bellanger M. CDMA transmission with complex OFDM/OQAM. *EURASIP J Wirel Commun Netw.* 2008;2008(18):1-12.
25. Lele C, Siohan P, Legouable R. The Alamouti scheme with CDMA-OFDM/OQAM. *EURASIP J Adv Signal Process* 2010. 2010; 2010(2):1-13.
26. Zakaria R, Le Ruyet D. A novel Filter-Bank multicarrier scheme to mitigate the intrinsic interference Application to MIMO systems. *IEEE Trans Wirel Commun.* 2012;2012(3):112-1123.

How to cite this article: Towliat M, Asgari Tabatabaee SMJ. On the time-frequency symbol density of FBMC/QAM systems. *Int J Commun Syst.* 2018;e3516. <https://doi.org/10.1002/dac.3516>

APPENDIX A

Consider the $\beta \times \beta$ matrix \mathbf{T} in (25), when $\mathbf{\Lambda} = \mathbf{F}_\beta^H \mathbf{T} \mathbf{F}_\beta$, the (n, q) th entry of $\mathbf{\Lambda}$ becomes

$$\begin{aligned}
 (\mathbf{\Lambda})_{n,q} = & \frac{1}{\beta} \left\{ \sum_{\substack{l_1=0 \\ \text{even } l_1}}^{\beta-1} \left[\sum_{\substack{l_2=0 \\ \text{even } l_2}}^{\beta-1} (\mathbf{T})_{l_1, l_2} e^{-j2\pi l_2 q / \beta} \right] e^{j2\pi l_1 n / \beta} \right. \\
 & + \sum_{\substack{l_1=0 \\ \text{odd } l_1}}^{\beta-1} \left[\sum_{\substack{l_2=0 \\ \text{odd } l_2}}^{\beta-1} (\mathbf{T})_{l_1, l_2} e^{-j2\pi l_2 q / \beta} \right] e^{j2\pi l_1 n / \beta} \\
 & + \sum_{\substack{l_1=0 \\ \text{odd } l_1}}^{\beta-1} \left[\sum_{\substack{l_2=0 \\ \text{even } l_2}}^{\beta-1} (\mathbf{T})_{l_1, l_2} e^{-j2\pi l_2 q / \beta} \right] e^{j2\pi l_1 n / \beta} \\
 & \left. + \sum_{\substack{l_1=0 \\ \text{even } l_1}}^{\beta-1} \left[\sum_{\substack{l_2=0 \\ \text{odd } l_2}}^{\beta-1} (\mathbf{T})_{l_1, l_2} e^{-j2\pi l_2 q / \beta} \right] e^{j2\pi l_1 n / \beta} \right\}. \tag{A1}
 \end{aligned}$$

From (25) and (26), it is easy to derive that (A1) can be rewritten as

$$\begin{aligned}
 \mathbf{\Lambda}_{(n,q)} = & \frac{1}{\beta} \left\{ \sum_{l_1=0}^{\beta/2-1} \left[\sum_{l_2=0}^{\beta/2-1} a_{[l_1-l_2]_{\beta/2}} e^{-j2\pi l_2 q / (\beta/2)} \right] e^{j2\pi l_1 n / (\beta/2)} \right. \\
 & + e^{j2\pi(n-q)/\beta} \sum_{l_1=0}^{\beta/2-1} \left[\sum_{l_2=0}^{\beta/2-1} b_{[l_1-l_2]_{\beta/2}} e^{-j2\pi l_2 q / (\beta/2)} \right] e^{j2\pi l_1 n / (\beta/2)} \\
 & + e^{j2\pi n / \beta} \sum_{l_1=0}^{\beta/2-1} \left[\sum_{l_2=0}^{\beta/2-1} c_{[l_1-l_2]_{\beta/2}} e^{-j2\pi l_2 q / (\beta/2)} \right] e^{j2\pi l_1 n / (\beta/2)} \\
 & \left. + e^{-j2\pi q / \beta} \sum_{l_1=0}^{\beta/2-1} \left[\sum_{l_2=0}^{\beta/2-1} d_{[l_1-l_2]_{\beta/2}} e^{-j2\pi l_2 q / (\beta/2)} \right] e^{j2\pi l_1 n / (\beta/2)} \right\}. \tag{A2}
 \end{aligned}$$

Then, we can write

$$\begin{aligned} \Lambda_{(n,q)} = & \frac{1}{\beta} \left\{ \sum_{l_1=0}^{\beta/2-1} a_{[l_1]_{\beta/2}} e^{j2\pi l_1 n / (\beta/2)} \sum_{l_2=0}^{\beta/2-1} e^{-j2\pi l_2 (q-n) / (\beta/2)} \right. \\ & + e^{j2\pi(n-q)/\beta} \sum_{l_1=0}^{\beta/2-1} b_{[l_1]_{\beta/2}} e^{j2\pi l_1 n / (\beta/2)} \sum_{l_2=0}^{\beta/2-1} e^{-j2\pi l_2 (q-n) / (\beta/2)} \\ & + e^{j2\pi n / \beta} \sum_{l_1=0}^{\beta/2-1} c_{[l_1]_{\beta/2}} e^{j2\pi l_1 n / (\beta/2)} \sum_{l_2=0}^{\beta/2-1} e^{-j2\pi l_2 (q-n) / (\beta/2)} \\ & \left. + e^{-j2\pi n / \beta} \sum_{l_1=0}^{\beta/2-1} d_{[l_1]_{\beta/2}} e^{j2\pi l_1 n / (\beta/2)} \sum_{l_2=0}^{\beta/2-1} e^{-j2\pi l_2 (q-n) / (\beta/2)} \right\}. \end{aligned} \quad (\text{A3})$$

According to (A3), $\Lambda_{(n,q)}$ is equivalent (28).

APPENDIX B

1) Proof of $\mathbf{A}'_n + \mathbf{B}'_n = \mathbf{I}_L$

In case of a well-localized prototype filter, for each $i \neq 0$, when Δl is even, we have $\xi_{2i,\ell}^+ = 0$, and also, it is always¹⁰ $\xi_{0,0}^+ = 1/2$. Accordingly, from (41), we can write

$$(\mathbf{A}'_n)_{p,p} + (\mathbf{B}'_n)_{p,p} = \sum_{i=0}^{N/2-1} \sum_{\Delta l=0}^{L-1} \left(\begin{array}{c} \xi_{[2i]_{N/2}, [\Delta l]_L}^+ \\ + (-1)^{\Delta l} \xi_{[2i]_{N/2}, [\Delta l]_L}^+ \end{array} \right) e^{j2\pi \Delta l p / L} e^{j2\pi i n / (N/2)} = 1, \quad (\text{B1})$$

where $n = 0, \dots, N-1$ and $p = 0, \dots, L-1$. Since \mathbf{A}'_n and \mathbf{B}'_n are diagonal, in matrix form, (B1) leads to $\mathbf{A}'_n + \mathbf{B}'_n = \mathbf{I}_L$.

2) Proof of $\mathbf{A}'_n - \mathbf{B}'_n = \mathbf{0}_L$

According to (B1), we have $(\mathbf{A}'_n)_{p,p} - (\mathbf{B}'_n)_{p,p} = 2(\mathbf{A}'_n)_{p,p} - 1$. Considering (10) into (41) leads to (B2).

$$\begin{aligned} (\mathbf{A}'_n)_{p,p} - (\mathbf{B}'_n)_{p,p} &= 2(\mathbf{A}'_n)_{p,p} - 1 \\ &= \sum_{i=0}^{N/2-1} \sum_{\Delta l=0}^{L-1} \left(\sum_{m=-\infty}^{\infty} f[m - L[i]_{N/2}] f[m] e^{-j2\pi \Delta l m / L} \right) e^{j2\pi \Delta l p / L} e^{j2\pi i n / (N/2)} - 1 \\ &= \sum_{i=0}^{N/2-1} \left(\sum_{m=-\infty}^{\infty} f[m - L[i]_{N/2}] f[m] \right) e^{j2\pi i n / (N/2)} \sum_{\Delta l=0}^{L-1} e^{-j2\pi \Delta l (m-p) / L} - 1. \end{aligned} \quad (\text{B2})$$

In (B2), the term $\sum_{\Delta l=0}^{L-1} e^{-j2\pi \Delta l (m-p) / L} = L$, if $m = vL + p$, and $\sum_{\Delta l=0}^{L-1} e^{-j2\pi \Delta l (m-p) / L} = 0$, if $m \neq vL + p$ (where v is an integer number). Thus, we can represent (B2) as

$$(\mathbf{A}'_n)_{p,p} - (\mathbf{B}'_n)_{p,p} = L \sum_{i=0}^{N/2-1} \left(\sum_{v=-\infty}^{\infty} f[(v + [i]_{N/2})L + p] f[vL + p] \right) e^{j2\pi i n / (N/2)} - 1. \quad (\text{B3})$$

On the other hand, for each well-localized prototype pulse-shape $f[m]$, for all values of p , we have¹⁰

$$L \sum_{v=-\infty}^{\infty} f[(v + [i]_{N/2})L + p] f[vL + p] = \begin{cases} 1; & \text{when } i = 0, \\ 0; & \text{when } i \neq 0. \end{cases} \quad (\text{B4})$$

As a result, for all values of $n = 0, \dots, N-1$ and $p = 0, \dots, L-1$, (B4) yields to

$$(\mathbf{A}'_n)_{p,p} - (\mathbf{B}'_n)_{p,p} = 0. \quad (\text{B5})$$

Since \mathbf{A}'_n and \mathbf{B}'_n are diagonal, in a matrix form, we have $\mathbf{A}'_n - \mathbf{B}'_n = \mathbf{0}_L$.

3) *Proof of $|\mathbf{C}'_n| = 1/2\mathbf{I}_L$*

In a similar way of the previous section, we can derive Equation B7. According to (B4), (B7) can be represented as

$$(\mathbf{C}'_n)_{p,p} = \frac{L}{2} \sum_{i=0}^{N/2-1} \left(\sum_{v=-\infty}^{\infty} f[(v + [i]_{N/2})L - L/2 + p] f[vL + p] \right) e^{j2\pi in/(N/2)} \quad (\text{B6})$$

$$= \frac{L}{2} \sum_{i=0}^{N/2-1} \left(\sum_{v=-\infty}^{\infty} f[(v + [i]_{N/2})L + p] f[vL + p] \right) e^{j2\pi in/(N/2)} e^{j2\pi Ln/N},$$

$$(\mathbf{C}'_n)_{p,p} = \frac{1}{2} e^{j2\pi Ln/N}. \quad (\text{B7})$$

Since \mathbf{C}'_n is diagonal, in a matrix form, it becomes $|\mathbf{C}'_n| = 1/2\mathbf{I}_L$.